Supplement of Geosci. Model Dev., 19, 1121–1141, 2026
https://doi.org/10.5194/gmd-19-1121-2026-supplement

Geoscientific Model Development
Open Access
EGU

Supplement of

Simulating the recent drought-induced mortality of European beech (*Fagus sylvatica* L.) and Norway spruce (*Picea abies* L.) in German forests

Gina Marano et al.

Correspondence to: Gina Marano (gina.marano@wsl.ch)

Supplementary Material 1

S1 | Climate data

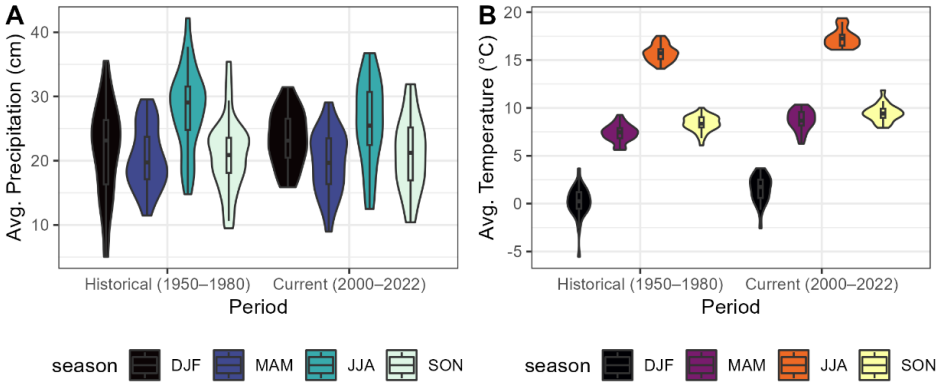

Figure S1 – Means of climatic variables (precipitation (A), temperature (B)) for the historical period (1950-1980) and the current climate period (2000-2022) averaged across the European beech-dominated sites.

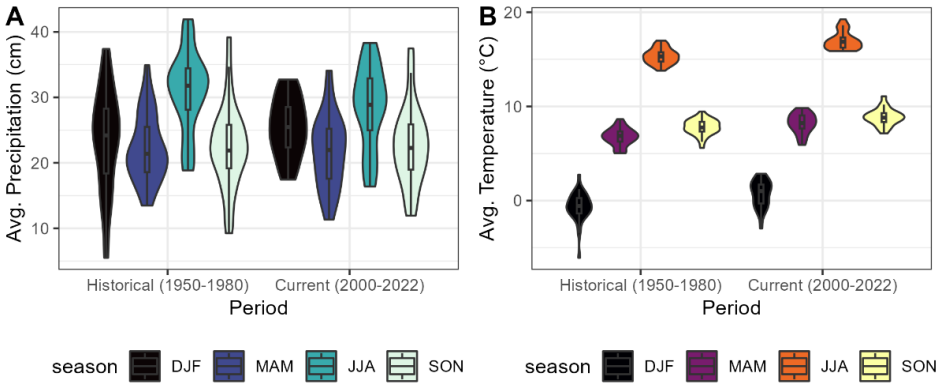

Figure S2 – Means of climatic variables (precipitation (A), temperature (B)) for the historical period (1950-1980) and the current climate period (2000-2022) averaged across the Norway spruce-dominated sites.

S2 | ForClim v.4.1

2.1 Maps of Available Water Capacity

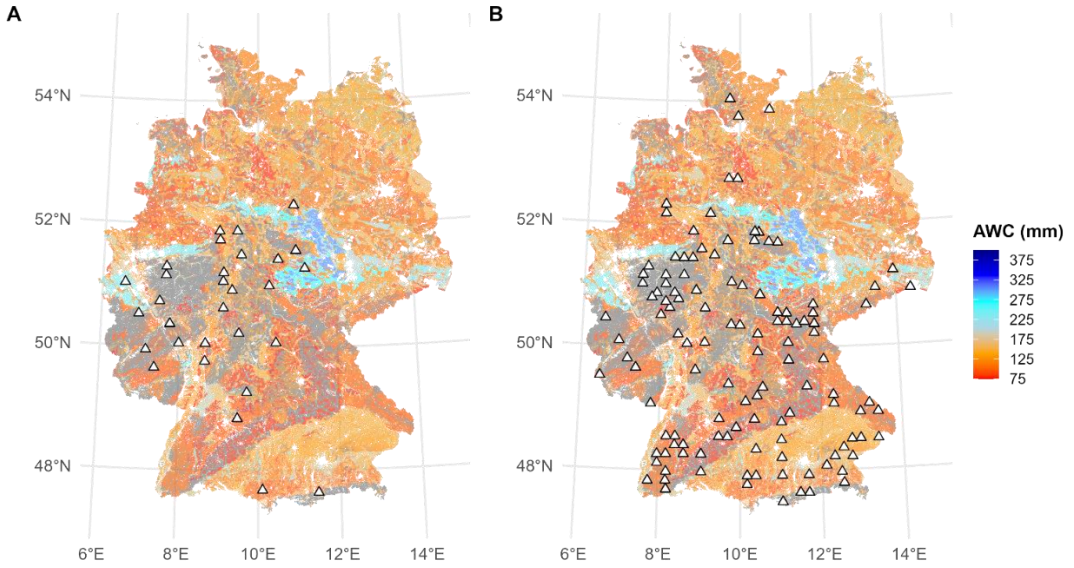

Figure S3 – Available Water Capacity (AWC, mm, source: BGD) maps and overlayed ICP Level I (WZE) plots dominated by European beech (**A**) and Norway spruce (**B**).

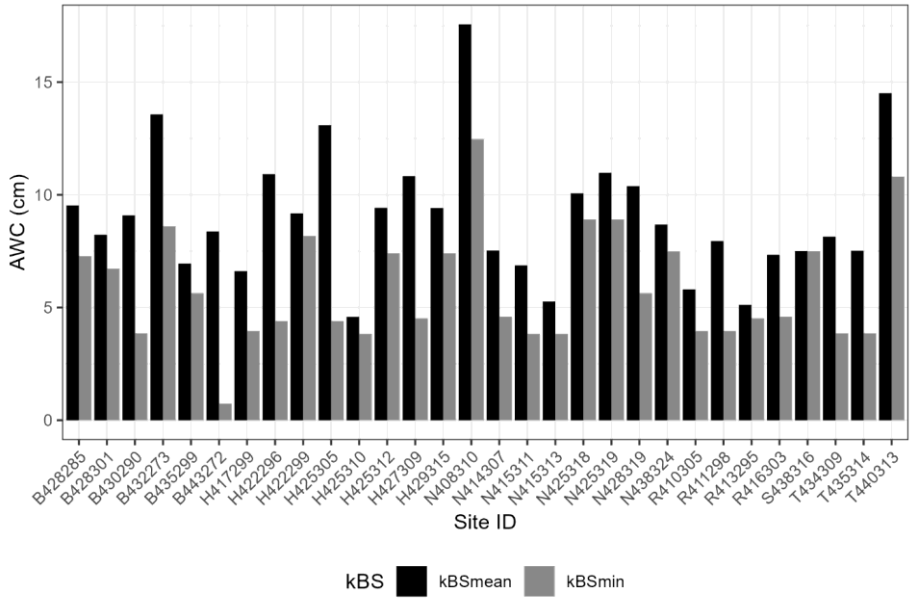

Figure S4 – AWC values (cm, mean and minimum) extracted from the BGR map across the ICP Level I beech-dominated sites.

Table S1 – Soil moisture scenarios defined according to kBS_{min} and kBS_{mean}. The heterogeneity of each scenario is expressed via the sigma values (σ) of the lognormal distribution.

Scenario	kBS_{min}	kBS_{mean}	σ
1	7.5	7.5	0
2	7.5	10	0.287
3	7.5	12.5	0.510
4	7.5	15	0.693
5	7.5	17.5	0.847
6	7.5	20	0.980
7	7.5	22.5	1.098
8	7.5	25	1.203
9	7.5	27.5	1.299
10	7.5	30	1.386
11	7.5	32.5	1.466
12	7.5	35	1.540
13	7.5	37.5	1.609
14	7.5	40	1.673
15	10	10	0
16	10	12.5	0.223
17	10	15	0.405
18	10	17.5	0.559
19	10	20	0.693
20	10	22.5	0.810
21	10	25	0.916
22	10	27.5	1.011
23	10	30	1.098
24	10	32.5	1.178
25	10	35	1.252
26	10	37.5	1.321
27	10	40	1.386
28	12.5	12.5	0
29	12.5	15	0.182
30	12.5	17.5	0.336
31	12.5	20	0.470
32	12.5	22.5	0.587
33	12.5	25	0.693
34	12.5	27.5	0.788
35	12.5	30	0.875
36	12.5	32.5	0.955
37	12.5	35	1.029
38	12.5	37.5	1.098
39	12.5	40	1.163
40	15	15	0
41	15	17.5	0.154
42	15	20	0.287
43	15	22.5	0.405
44	15	25	0.510
45	15	27.5	0.606
46	15	30	0.693
47	15	32.5	0.773
48	15	35	0.847
49	15	37.5	0.916
50	15	40	0.980
51	17.5	17.5	0
52	17.5	20	0.133
53	17.5	22.5	0.251
54	17.5	25	0.356
55	17.5	27.5	0.451
56	17.5	30	0.538
57	17.5	32.5	0.619
58	17.5	35	0.693
59	17.5	37.5	0.762
60	17.5	40	0.826
61	20	20	0
62	20	22.5	0.117
63	20	25	0.223
64	20	27.5	0.318
65	20	30	0.405
66	20	32.5	0.485
67	20	35	0.559
68	20	37.5	0.628
69	20	40	0.693
70	22.5	22.5	0
71	22.5	25	0.105
72	22.5	27.5	0.200
73	22.5	30	0.287
74	22.5	32.5	0.367
75	22.5	35	0.441
76	22.5	37.5	0.510
77	22.5	40	0.575
78	25	25	0
79	25	27.5	0.095
80	25	30	0.182
81	25	32.5	0.262
82	25	35	0.336
83	25	37.5	0.405
84	25	40	0.470
85	27.5	27.5	0
86	27.5	30	0.087
87	27.5	32.5	0.167
88	27.5	35	0.241
89	27.5	37.5	0.310
90	27.5	40	0.374
91	30	30	0
92	30	32.5	0.080
93	30	35	0.154
94	30	37.5	0.223
95	30	40	0.287
96	32.5	32.5	0
97	32.5	35	0.074
98	32.5	37.5	0.143
99	32.5	40	0.207
100	35	35	0
101	35	37.5	0.068
102	35	40	0.133
103	37.5	37.5	0
104	37.5	40	0.064
105	40	40	0

2.2 Spatial heterogeneity level (σ) of soil moisture and model performance

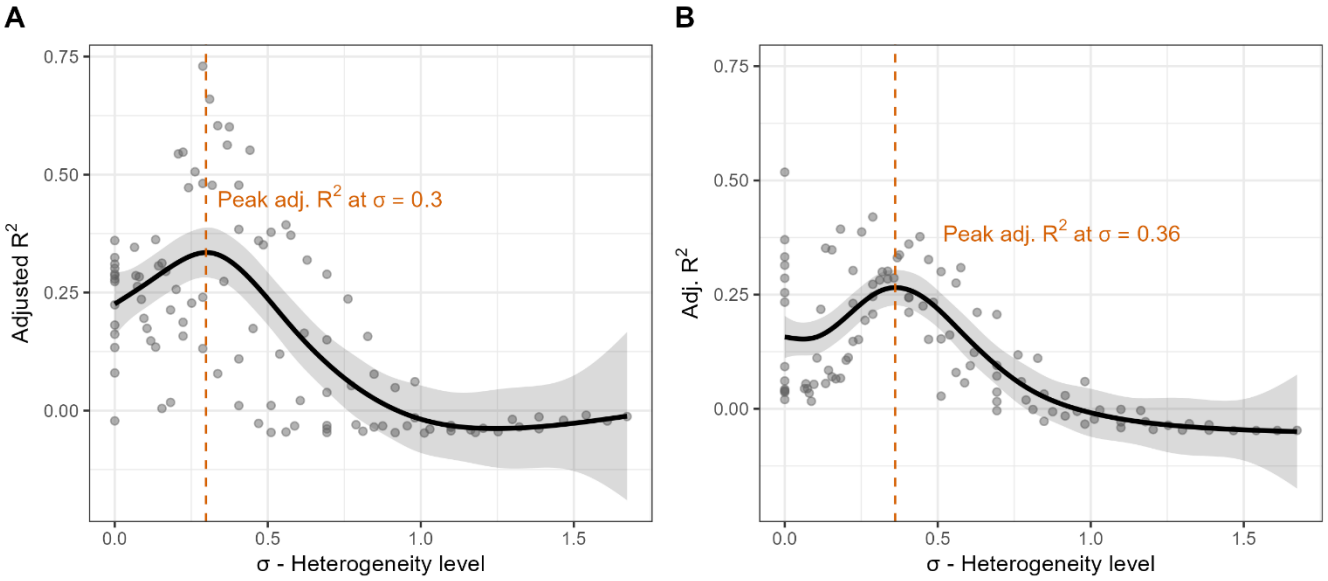

Figure S5 – Relationship between heterogeneity level of soil moisture (σ) and model performance (Adjusted R^2) for *Fagus sylvatica* (**A**) and *Picea abies* (**B**). A generalized additive model (GAM) was fitted to predict R^2 as a smooth function of σ. The shaded area indicates the 95% confidence interval of the GAM. Model performance peaked at $\sigma \approx 0.3$ and 0.36, respectively, for *Fagus sylvatica* and for *Picea abies* and declined thereafter, suggesting optimal model fit under intermediate (*Fagus*) and more pronounced (*Picea*) heterogeneity levels.

Table S2 - Summary of Generalized Additive Models (GAMs) fitted to predict adjusted R^2 as a function of soil moisture heterogeneity (σ) for *Fagus sylvatica* and *Picea abies*. edf = estimated degrees of freedom, red.df = reference degrees of freedom. Parametric and smooth term estimates are provided along with model statistics including adjusted R^2, deviance explained (D), restricted maximum likelihood (REML), scale estimate (scale), and sample size (*n*). All smooth terms were highly significant ($p < 0.001$). All GAMs were fitted using a Gaussian family with an identity link function.

Species						
Fagus sylvatica	**Parametric term**	*Component*	*Estimate*	*Std. error*	*t-value*	*p-value*
		Intercept	0.2	0.01	12.5	<2e-16
	Smooth term		*edf*	*red.df.*	*F-value*	
		σ	4.4	9	9.9	<2e-16
	Model statistics					
	adj. R^2	*D*	*REML*	*scale*	*n*	
	0.46	48.4%	-41.7	0.02	105	
Picea abies	**Parametric term**	*Component*	*Estimate*	*Std. error*	*t-value*	
		Intercept	0.1	0.01	14.1	<2e-16
	Smooth term		*edf*	*red.df.*	*F-value*	
		σ	5.5	9	13.3	<2e-16
	Model statistics					
	adj. R^2	*D*	*REML*	*scale*	*n*	
	0.53	55.9%	-83.2	0.01	105	

2.3 Base annual probability of Bark beetle outbreaks

We derived the base annual probability of bark beetle outbreaks (P_{bark}) by adapting the theoretical probability of bark beetle disturbance in spruce-dominated forests (Hlásny et al., 2021, their Fig. 4 and Appendix 2) to baseline climate conditions (1979–1990) in Germany. The method we used combined fixed percentages for the lower classes and an exponential progression for the higher classes, as follows:

1. *No Spruce*: this category represents the absence of spruce; hence the base probability of a bark beetle outbreak is 0%.
2. *Very Low*: we assigned to this class the first 5% of the range to capture very rare occurrences of bark beetle attacks.
3. *Low*: this category covers the next 10% (from 6 to 15%), which reflects low but non-negligible occurrences of outbreaks.
4. *Medium, High,* and *Very High:* the remaining 85% of the scale (from 16 to 100%) was divided between the three categories using an exponential progression. This approach was chosen to smoothly reflect the increasing intensity or abundance of spruce, with progressively larger ranges as we move towards the higher classes. Furthermore, it ensures that the higher classes have larger ranges, which is appropriate for a classification where higher abundances are typically more variable.

The progression was defined using a base factor that determines how the range grows as we move from one class to the next. The exponential progression R_k (Eq. S1) represents the upper range limit of the kth class, with $k = 1, 2, 3$, which corresponds to the *Medium*, *High*, and *Very High* classes, respectively. R_0 represents the initial range size (i.e., 19 units for *Medium*, 31 units for *High* and 35 units for *Very High*), λ is the exponential growth factor and k is the class index.

$$R_{\mathrm{k}} = R_0 \cdot \lambda^k \quad \text{(S1)}$$

Given that the total span for the upper classes must equal to 85 units (i.e., covering the range [16,100]), we selected $\lambda = 1.5$ which ensures that the cumulative ranges (i.e. 19 + 31 + 35 = 85) cover the full interval. The value $\lambda = 1.5$ thus controls the exponential increase in range width from *Medium* to *Very High*. The range [16,100] is therefore split into three sections such that the total span is covered by the classes with exponentially increasing intervals.

Table S3 - Base annual probability for the six bark beetle outbreak classes with estimated ranges and midpoints. The original class definitions are derived from Hlasny et al. (2021).

Class	Range (%)	Midpoint (%)
No spruce	0	0
Very Low	0-5	2.5
Low	6-15	10.5
Medium	16-34	25
High	35-65	50
Very High	66-100	83

S3 | Stand Data

3.1 | ICP Level I data overview

3.1.1. Beech sites

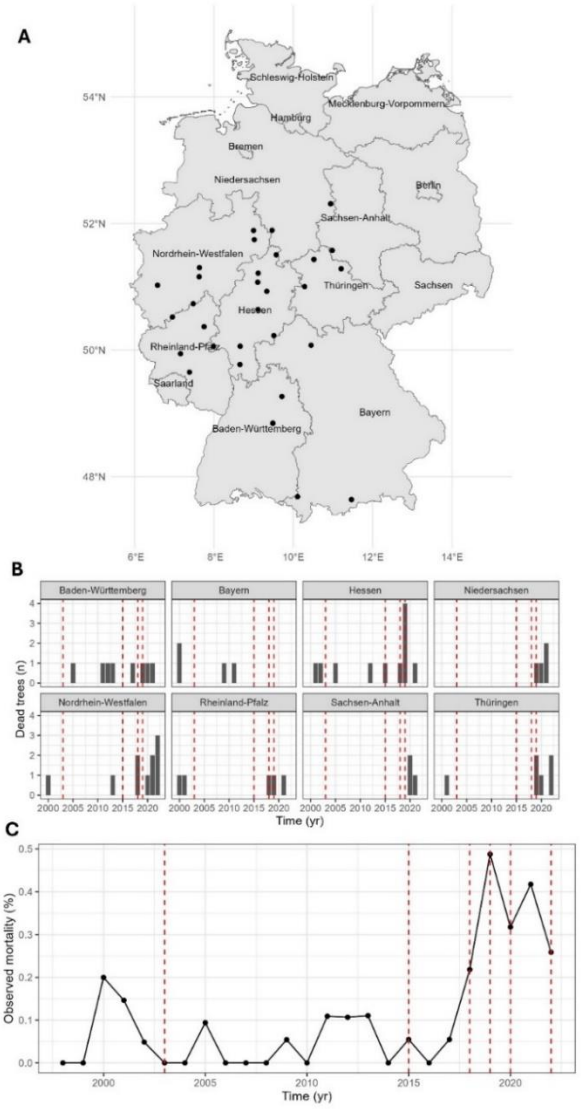

Figure S6 – (**A**) Locations of ICP Forest Level I network plots in European beech (*Fagus sylvatica L.*)–dominated stands across the study region. (**B**) Total number of dead beech trees recorded within these plots over the observation period. (C) Observed mortality rate of beech trees, derived from repeated assessments at the same network plots.

3.1.2. Spruce sites

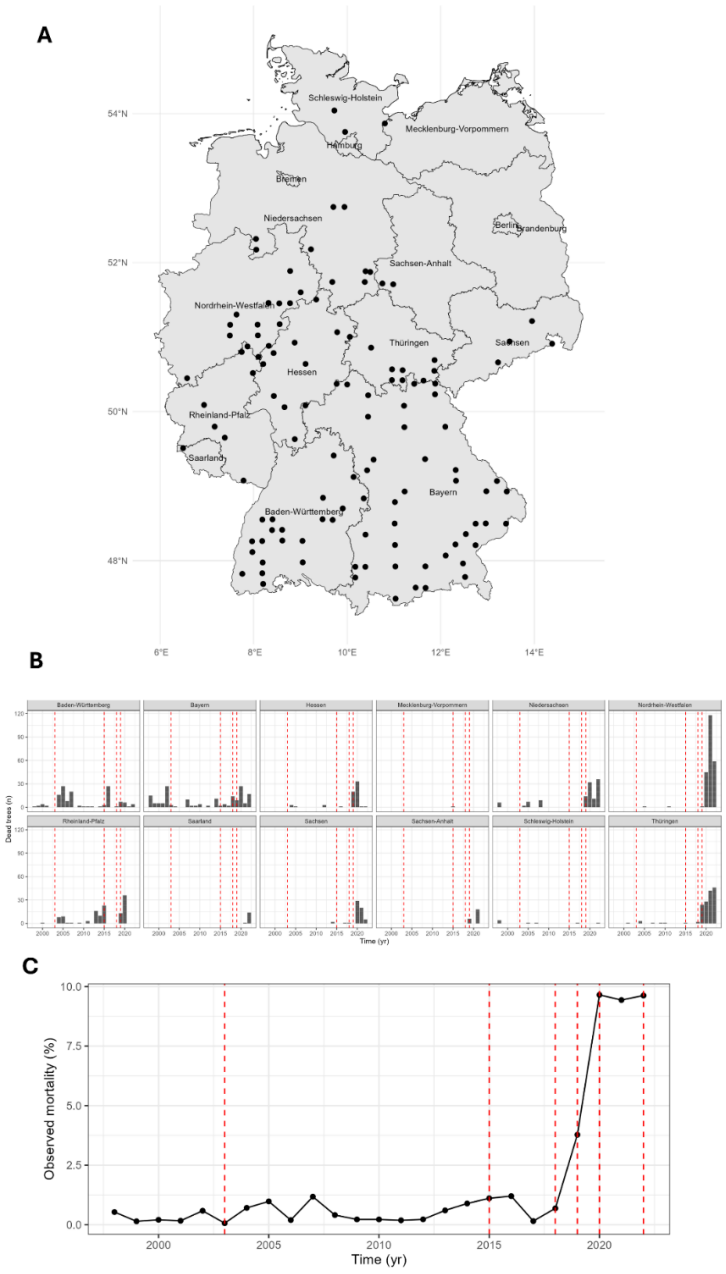

65 *Figure S7* – (**A**) Locations of ICP Forest Level I network plots in Norway spruce (*Picea abies L.*)–dominated stands across the study region. (**B**) Total number of dead beech trees recorded within these plots over the observation period. (C) Observed mortality rate of beech trees, derived from repeated assessments at the same network plots.

3.2 | Stand-level mortality and Drought index

3.2.1. Beech sites

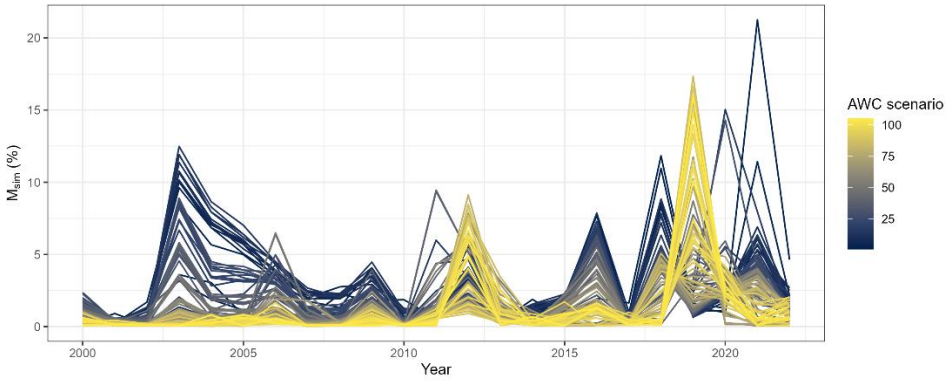

Figure S8 – Simulated mortality rate over time averaged across beech sites and grouped by soil scenario. We only show trees with a DBH > 40 cm.

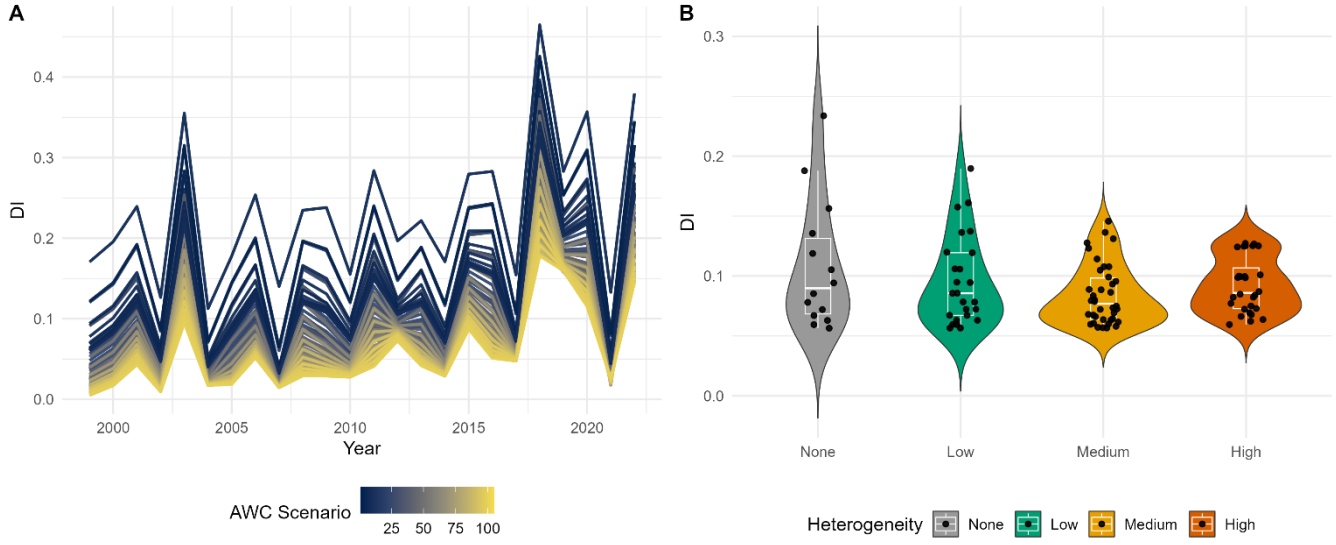

Figure S9 – (**A**) ForClim drought index calculated at the seasonal (i.e. April-October, growing season) timestep for each AWC scenario, (**B**) and aggregated across heterogeneity classes.

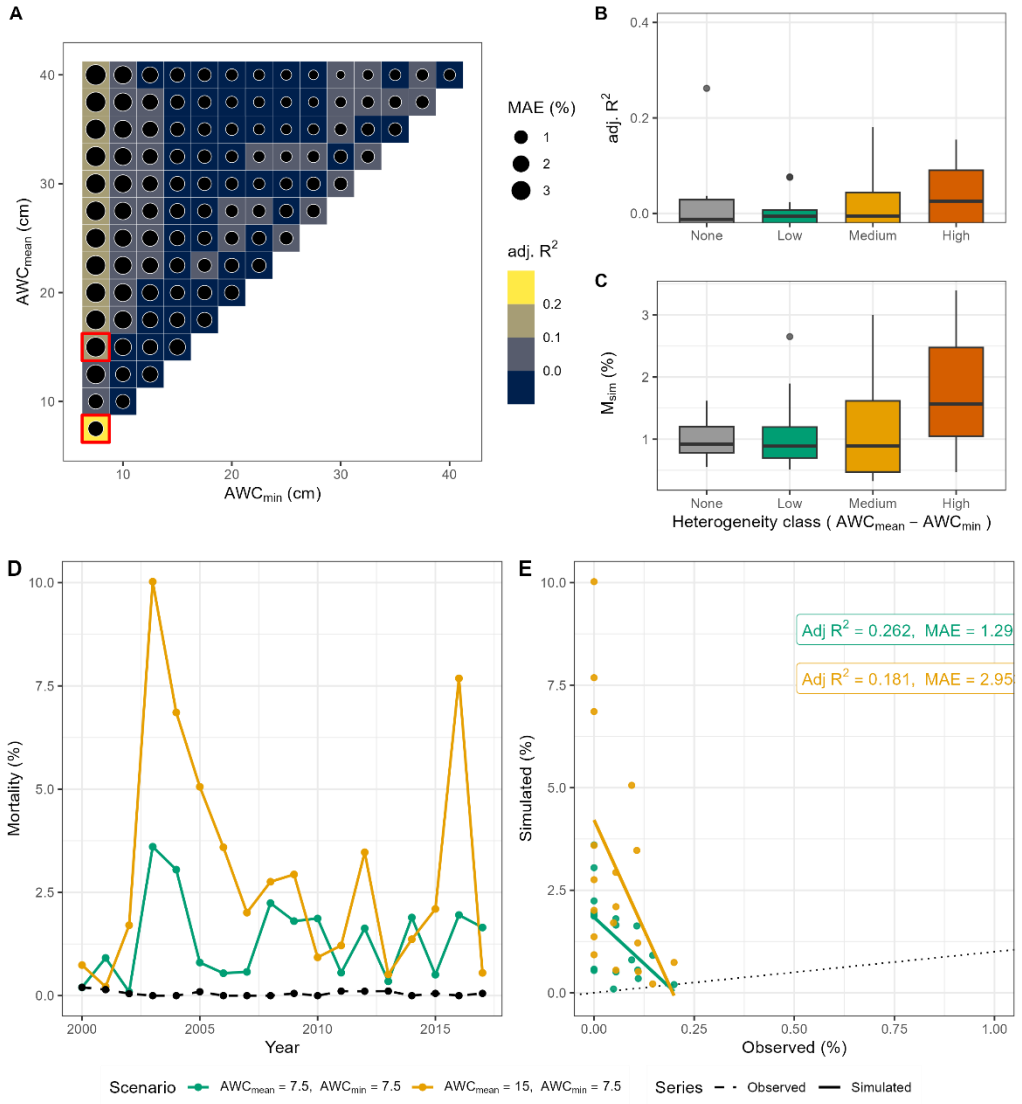

Figure S10 – Evaluation of the performance of soil moisture scenarios in reproducing simulated tree mortality compared to observed tree mortality for European beech-dominated sites when using the 2000-2017 period only. (**A**) AWC scenarios showing adjusted R^2 and MAE. The two top-ranked AWC scenarios are indicated by red boxes. The lowermost highlighted box (in column 1) is scenario 1, while the other highlighted box in this column is scenario 4. (**B**) Adjusted R^2 and simulated mortality rate across heterogeneity classes (cf. Fig. 2, main manuscript). (**C**) Mean simulated mortality rate across heterogeneity classes. (**D**) Simulated (the two top-ranked AWC scenarios) and observed annual mortality rates over time across all sites, and (**E**) model statistics for the two top-ranked AWC scenarios.

3.2.2. Spruce sites

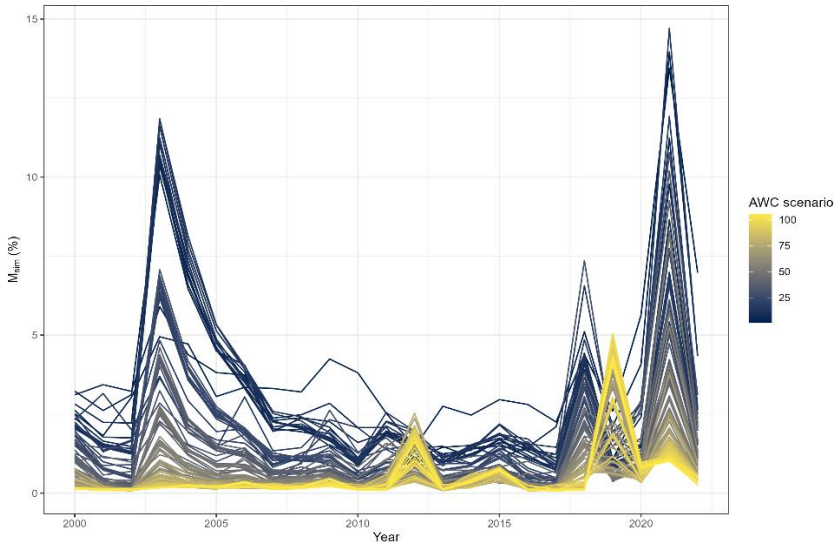

Figure S11 – Simulated mortality rate over time averaged across spruce sites and grouped soil scenario. We only show trees with a DBH > 40 cm.

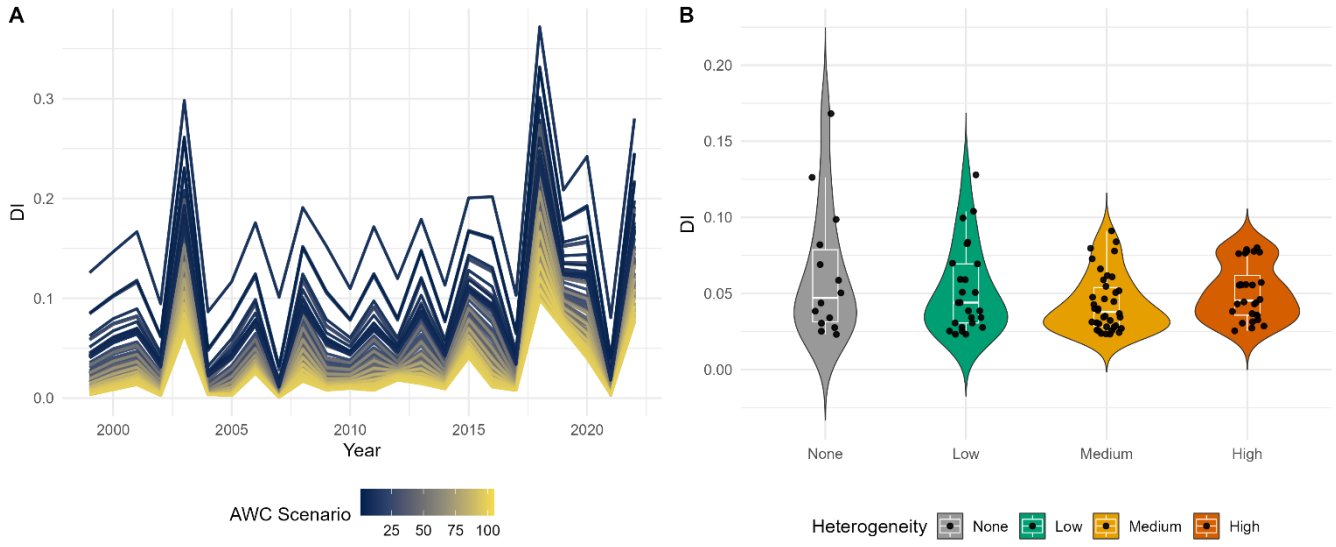

Figure S12 – (**A**) ForClim drought index calculated at the yearly timestep for each AWC scenario, (**B**) and aggregated across heterogeneity classes.

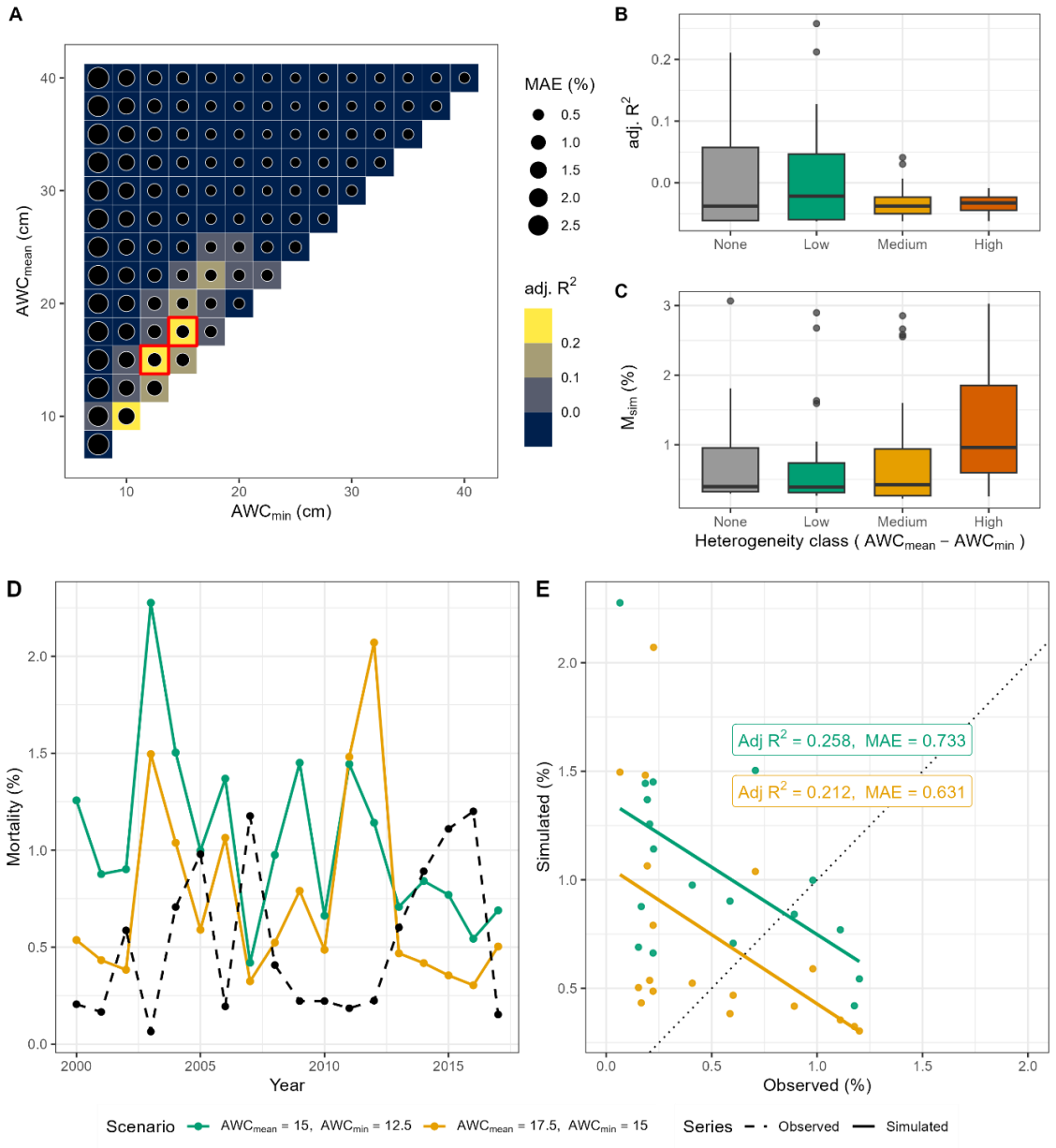

95 *Figure S13* – Evaluation of the performance of soil moisture scenarios in reproducing simulated tree mortality compared to observed tree mortality for Norway spruce-dominated sites when using the 2000-2017 period only. (**A**) AWC scenarios showing adjusted R^2 and MAE. The two top-ranked AWC scenarios are indicated by red boxes. The highlighted boxin the third column represents scenario 29, while the highlighted box in the fourth column represents scenario 41. (**B**) Adjusted R^2 and simulated mortality rate across heterogeneity classes (cf. Fig. 2, main manuscript). (**C**) Mean simulated mortality rate across
100 heterogeneity classes. (**D**) Simulated (the two top-ranked AWC scenarios) and observed annual mortality rates over time across all sites, and (**E**) model statistics for the two top-ranked AWC scenarios

3.3 | Mechanistic understanding of mortality: periods, PIC, spatial patterns

3.3.1 Mortality period

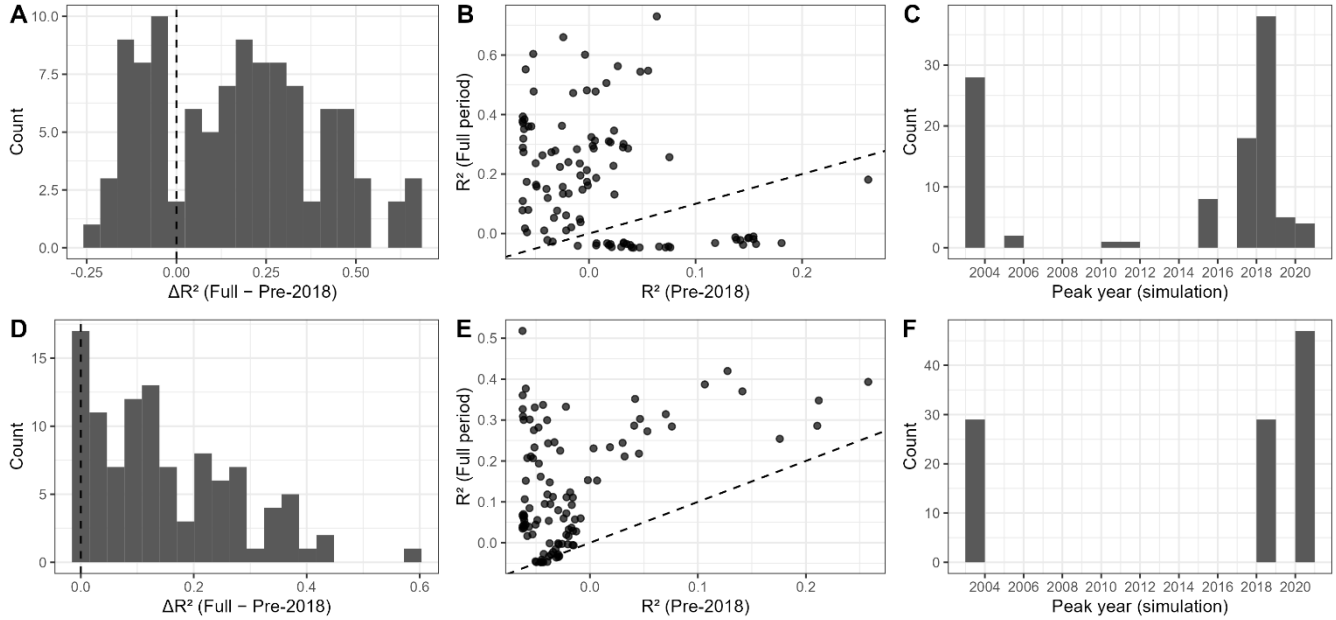

Figure S14 – Comparison of model performance and simulated mortality timing for *Fagus sylvatica* (**A–C**) and *Picea abies* (**D–F**) when evaluated for the full simulation period (2000–2022) versus the pre-2018 period. (**A, D**) Distribution of changes in explanatory power ($\Delta R^2 = R^2_{full} - R^2_{pre\text{-}2018}$) across the 105 AWC scenarios. Positive values indicate improved model performance when including the post-2017 drought years. (**B, E**) Relationship between model performance for the full period and the pre-2018 period; the 1:1 line (dashed) denotes equal explanatory power. Most scenarios lie above this line, showing that the extreme drought years enhance model discrimination rather than biasing fit statistics. (**C, F**) Distribution of simulated mortality peak years across AWC scenarios.

3.3.2 Predisposing and inciting factors

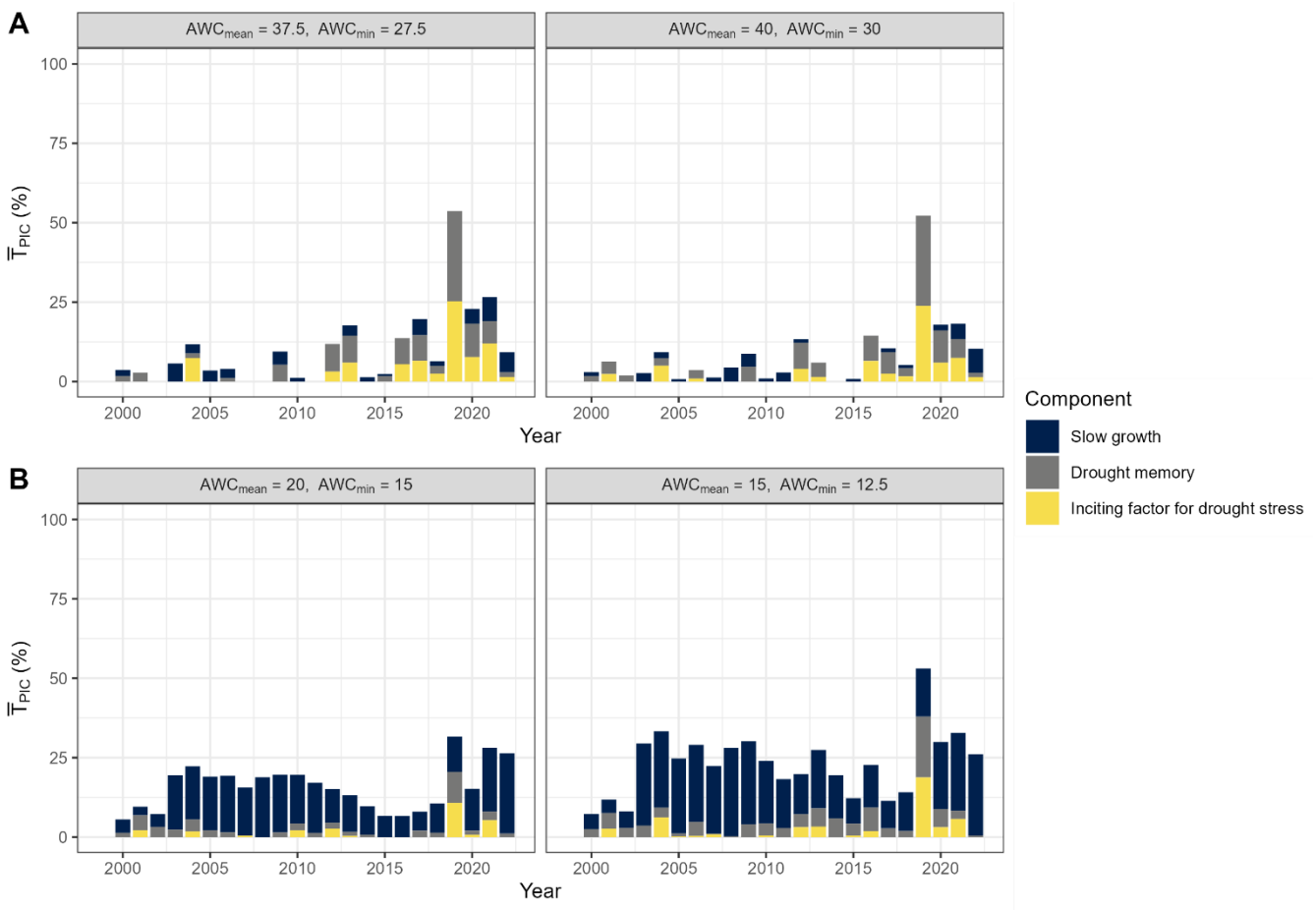

Figure S15 – Fraction of dead trees affected by predisposing and inciting stress factors ($\bar{T}_{PIC}$, %) simulated by ForClim v4.2 for (**A**) *Fagus sylvatica* and (**B**) *Picea abies* across two soil water availability scenarios. Bars represent annual stand-level averages of trees flagged for (i) slow growth (dark blue), (ii) drought memory (grey), and (iii) inciting drought stress (yellow). Each panel corresponds to the best performing AWC scenario, i.e. scenarios 89 and 95 for *Fagus sylvatica* and 29 and 42 for *Picea abies*, resulting from the combination of mean and minimum available water capacity, representing different levels of soil water storage and its local spatial heterogeneity. **Note**: the figure shows only the fraction of dead trees with DBH ≥ 40 cm that were flagged by the PIC model for stress-related mortality; other mortality (e.g., stochastic/background) and other size classes are not displayed.

3.3.3 Spatial mortality

To assess whether observed and simulated spruce mortality exhibited spatial patterns, we quantified spatial autocorrelation using both global and local statistics. All analyses were performed in R (version ≥ 4.3) with the packages *sf*, *spdep*, and *ggplot2*. Site coordinates were projected in the ETRS89–LAEA Europe coordinate system (EPSG 3035), and spatial relationships were defined using a 5-nearest-neighbour (kNN) weighting scheme based on Euclidean distances. Global spatial autocorrelation was evaluated with Moran's I ((Moran, 1950)), computed from 999 random permutations of mortality values. This statistic measures the similarity of nearby observations, with positive values indicating spatial clustering, zero corresponding to random spatial structure, and negative values indicating spatial dispersion. Local Indicators of Spatial Association (LISA; Anselin, 1995) were used to map site-level clusters of high or low mortality. Sites with significant ($p < 0.05$) local Moran's I values were classified as "High–High," "Low–Low," "High–Low," or "Low–High." For European beech, both observed and simulated mortality showed very weak and non-significant global autocorrelation (Observed $I = 0.06$, $p = 0.11$; Simulated $I = -0.13$, $p = 0.88$ (Figure S16, B). Only one small, non-significant "High–High" cluster was detected, indicating largely random spatial distribution (Figure S16, C). Together, these results demonstrate the absence of coherent spatial structure in both observed and simulated beech mortality, consistent with stochastic mortality processes and broad-scale environmental drivers rather than localized spatial effects. For Norway spruce, both observed and simulated mortality exhibited weak but statistically significant positive spatial autocorrelation (Observed $I = 0.15$, $p = 0.005$; Simulated $I = 0.09$, $p = 0.024$; Figure S17, B). This indicates that sites with high or low spruce mortality tended to be located near other sites with similar mortality levels, although the strength of this clustering was modest. The LISA revealed a few small but distinct "High–High" and "Low–Low" clusters of observed mortality, mainly concentrated in central and southern Germany (Figure S17, C). In contrast, simulated mortality showed only sparse and spatially inconsistent local clusters (Figure S17, D). Overall, these results suggest that observed spruce mortality exhibited weak but significant spatial aggregation, possibly reflecting regionally coherent environmental stressors or disturbance legacies (e.g., bark beetle outbreaks), whereas simulated mortality reproduced the general magnitude of mortality but not its localized spatial structure.

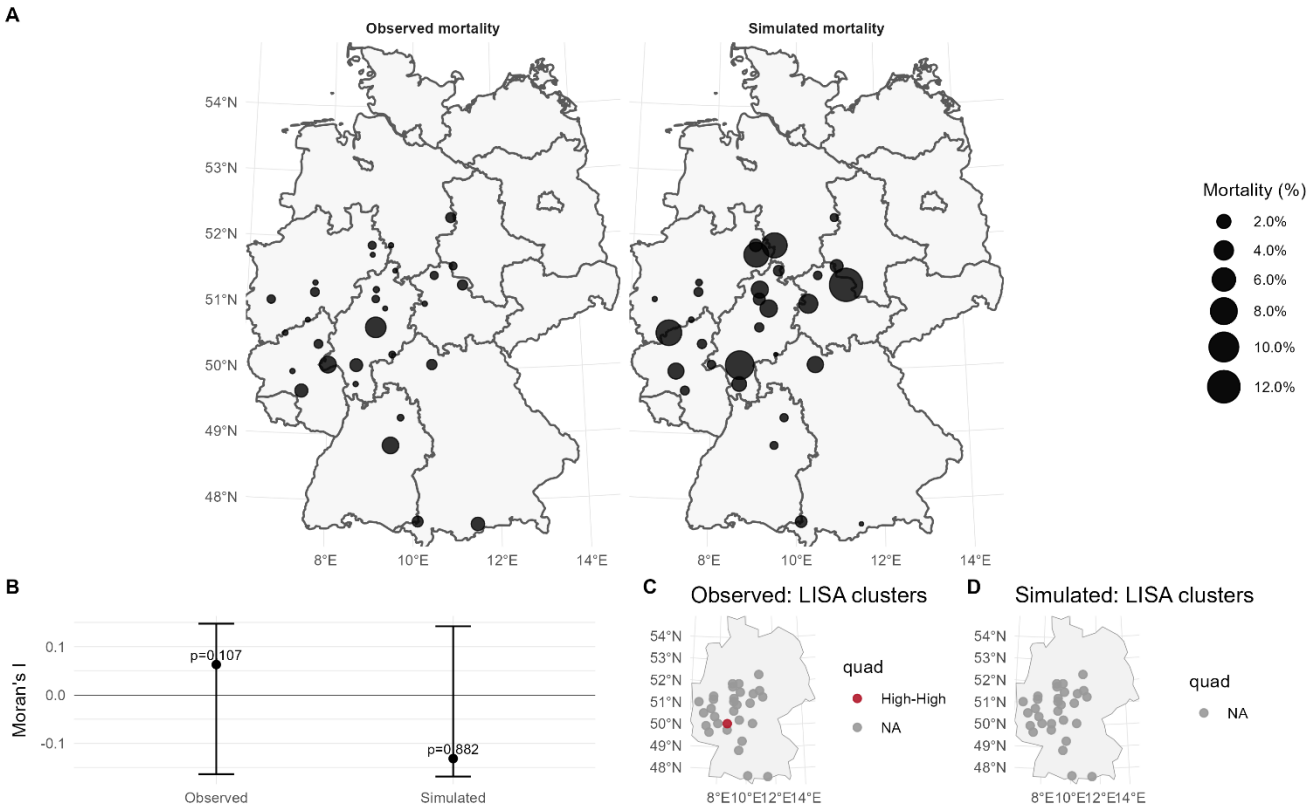

Figure S16 – **(A)** Maps of observed (left) and simulated (right) mean mortality (%) across all European beech dominated ICP-Level I monitoring sites in Germany. Circle size is proportional to site-level mortality. **(B)** Global spatial autocorrelation (Moran's I, 999 permutations, 5-nearest-neighbour weighting). Both observed (I = 0.06, p = 0.11) and simulated (I = –0.13, p = 0.88) mortality show no significant spatial autocorrelation.**(C–D)** Local Indicators of Spatial Association (LISA) cluster maps for observed (**C**) and simulated (**D**) mortality.

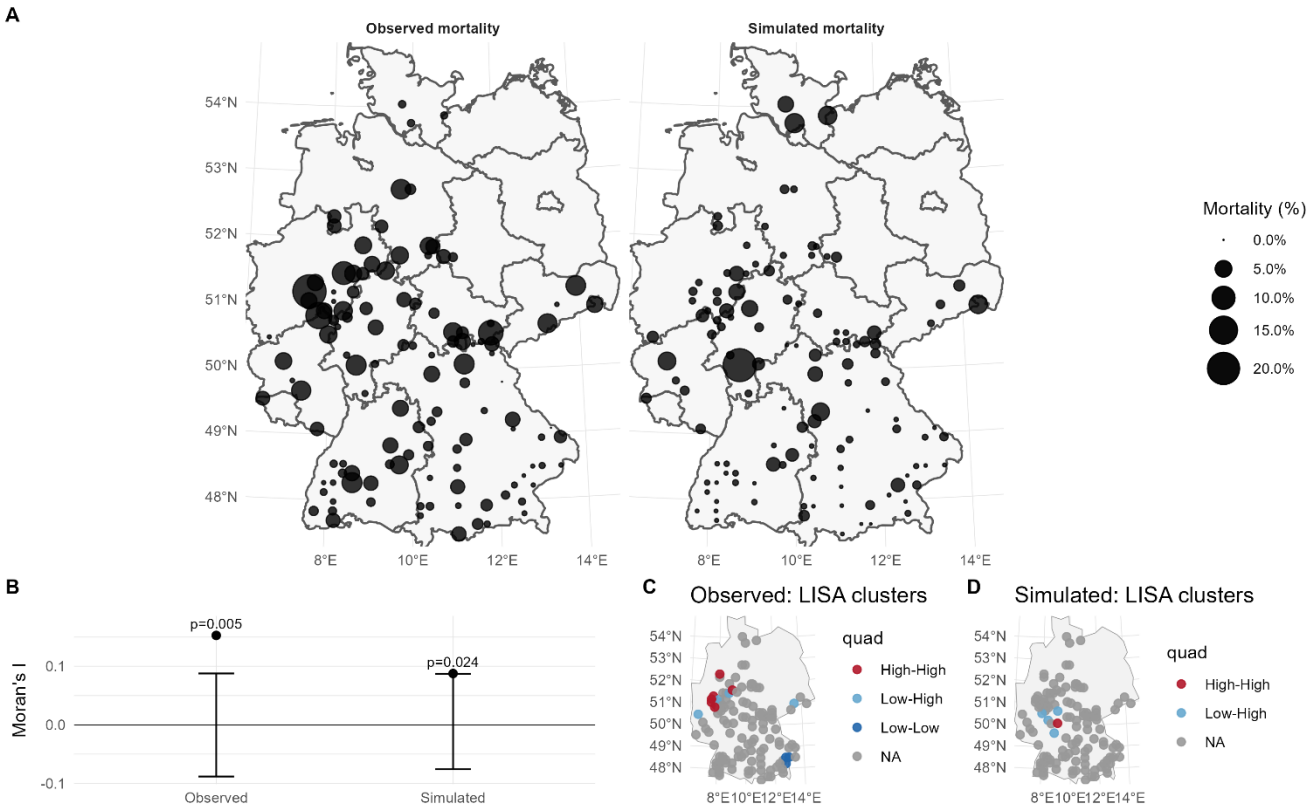

Figure S17 – **(A)** Maps of observed (left) and simulated (right) mean mortality (%) across all Norway spruce dominated ICP-Level I monitoring sites in Germany. Circle size is proportional to site-level mortality. **(B)** Global spatial autocorrelation (Moran's I, 999 permutations, 5-nearest-neighbour weighting). Both observed (I = 0.06, p = 0.11) and simulated (I = –0.13, p = 0.88) mortality show no significant spatial autocorrelation.**(C–D)** Local Indicators of Spatial Association (LISA) cluster maps for observed (**C**) and simulated (**D**) mortality.

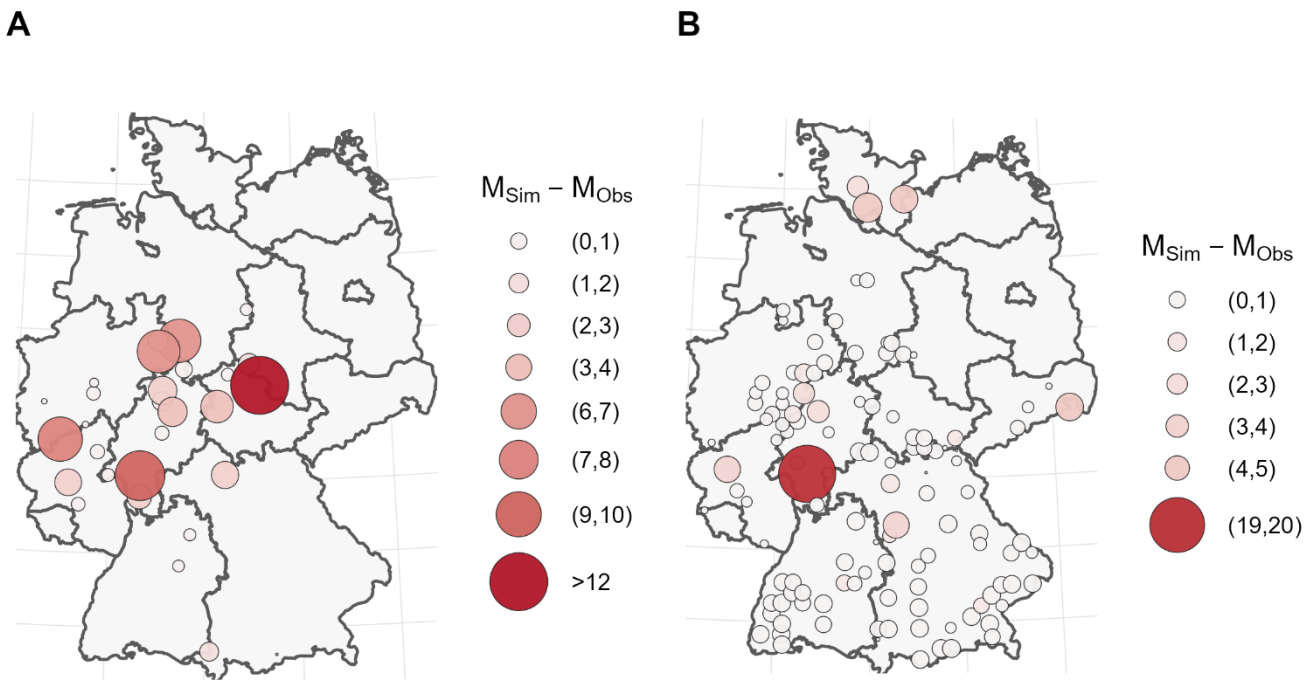

Figure S18 – Absolute difference between simulated and observed mortality rates averaged over the period 2000–2022 for each **(A)** beech-dominated and **(B)** spruce-dominated site for dominant trees (DBH > 40 cm). Circle size and color intensity indicate the magnitude of the absolute difference between simulated and observed mortality rates. Lighter colors and smaller circles represent smaller deviations, while darker and larger circles represent larger deviations. Classes not shown in the legend are empty. For beech 15 sites fell within the lowest overestimation class (0–1%), while only a few sites (n = 4 each) showed moderate overestimation (1–3%). Higher discrepancies (>6%) however occurred only at isolated locations (n = 4), indicating that substantial overprediction was spatially limited.

3.3.4. Scenario-specific model performance for the beech sites

Table S4 – Summary of the model statistics (MAE, RMSE, R^2_{adj}, Slope, Intercept and P-value) for each scenario for the beech dominated sites. Highlighted in red are the two best performing scenarios according to their R^2_{adj}.

Scenario	MAE	RMSE	R^2_{adj}	Slope	Intercept	P-Value
1	2.548	5.036	0.181	15.545	0.953	0.025
2	1.962	3.394	0.131	8.829	1.088	0.050
3	2.792	3.817	-0.046	-0.681	2.974	0.876
4	3.076	4.185	-0.032	-2.614	3.479	0.576
5	3.093	4.178	-0.035	-2.333	3.461	0.617

6	3.019	4.213	-0.015	-3.869	3.559	0.424
7	3.041	4.129	-0.032	-2.591	3.441	0.575
8	3.057	4.243	-0.038	-2.143	3.410	0.658
9	2.918	4.090	-0.019	-3.545	3.429	0.449
10	3.001	4.176	-0.014	-3.902	3.551	0.411
11	3.138	4.373	-0.020	-3.660	3.662	0.463
12	3.196	4.456	-0.010	-4.396	3.804	0.385
13	3.207	4.540	-0.022	-3.752	3.739	0.477
14	3.380	4.753	-0.013	-4.563	4.006	0.404
15	2.087	4.051	0.273	14.834	0.573	0.006
16	1.548	2.312	0.158	5.882	1.004	0.034
17	2.089	2.667	0.010	2.962	1.865	0.279
18	2.262	2.906	-0.045	-0.617	2.443	0.837
19	2.326	3.125	-0.046	-0.519	2.495	0.881
20	2.203	3.010	-0.044	-0.923	2.418	0.784
21	2.203	2.987	-0.047	-0.421	2.363	0.899
22	2.133	2.936	-0.048	0.014	2.244	0.997
23	2.246	3.126	-0.043	-1.084	2.481	0.761
24	2.210	3.013	-0.046	-0.522	2.383	0.876
25	2.285	3.131	-0.045	-0.807	2.490	0.818
26	2.314	3.197	-0.035	-1.808	2.631	0.615
27	2.277	3.152	-0.039	-1.501	2.560	0.673
28	2.066	3.871	0.134	10.429	1.026	0.048
29	1.435	2.297	0.017	3.398	1.162	0.252
30	1.608	2.187	0.078	3.919	1.278	0.105
31	1.687	2.221	-0.027	1.511	1.630	0.526
32	1.777	2.379	-0.033	1.419	1.730	0.587
33	1.712	2.348	-0.039	1.099	1.701	0.679
34	1.652	2.301	-0.030	1.564	1.589	0.556
35	1.671	2.293	-0.033	1.410	1.625	0.587
36	1.586	2.150	-0.032	1.310	1.552	0.584
37	1.644	2.231	-0.040	0.985	1.646	0.692
38	1.699	2.256	-0.035	1.196	1.677	0.625
39	1.632	2.213	-0.041	0.887	1.645	0.718
40	1.610	2.882	-0.022	2.848	1.388	0.474
41	1.325	2.385	0.004	3.357	1.035	0.307
42	1.310	2.035	0.240	6.301	0.709	0.010
43	1.448	1.898	0.109	3.660	1.146	0.068
44	1.466	1.981	0.011	2.387	1.310	0.279
45	1.429	1.958	0.021	2.602	1.248	0.238

46	1.375	1.894	0.038	2.843	1.167	0.186
47	1.353	1.867	0.053	3.050	1.122	0.151
48	1.285	1.808	0.077	3.365	1.018	0.107
49	1.206	1.678	0.049	2.695	1.013	0.160
50	1.295	1.765	0.061	2.957	1.074	0.134
51	1.403	2.656	0.080	6.011	0.796	0.103
52	1.230	2.351	0.134	6.419	0.581	0.048
53	1.139	2.064	0.228	6.834	0.445	0.012
54	1.245	1.695	0.274	5.017	0.784	0.006
55	1.272	1.755	0.174	4.320	0.897	0.027
56	1.073	1.462	0.120	3.083	0.838	0.059
57	1.146	1.591	0.164	3.865	0.822	0.031
58	1.066	1.534	0.150	3.730	0.759	0.038
59	1.084	1.559	0.236	4.574	0.680	0.011
60	1.017	1.432	0.157	3.471	0.737	0.035
61	1.403	2.857	0.162	8.541	0.504	0.032
62	1.256	2.712	0.148	7.915	0.425	0.040
63	1.108	2.043	0.187	6.325	0.462	0.023
64	1.023	1.621	0.477	7.070	0.331	0.000
65	0.999	1.412	0.384	5.114	0.530	0.001
66	0.898	1.320	0.351	4.762	0.470	0.002
67	0.954	1.366	0.393	5.096	0.489	0.001
68	0.876	1.366	0.319	4.920	0.432	0.003
69	0.900	1.392	0.289	4.756	0.474	0.005
70	1.436	3.556	0.224	12.630	0.079	0.013
71	1.188	2.689	0.174	8.489	0.326	0.027
72	0.985	1.994	0.257	7.236	0.262	0.008
73	0.905	1.608	0.481	7.464	0.162	0.000
74	0.840	1.260	0.563	5.861	0.284	0.000
75	0.851	1.310	0.552	6.100	0.268	0.000
76	0.789	1.243	0.378	4.904	0.345	0.001
77	0.809	1.309	0.371	5.184	0.333	0.001
78	1.359	3.507	0.301	14.298	-0.150	0.004
79	1.167	2.761	0.195	9.231	0.229	0.020
80	0.850	1.896	0.213	6.556	0.179	0.015
81	0.855	1.560	0.506	7.501	0.107	0.000
82	0.760	1.217	0.604	6.128	0.174	0.000
83	0.763	1.225	0.478	5.472	0.252	0.000
84	0.761	1.295	0.360	5.194	0.284	0.001
85	1.475	3.957	0.310	16.400	-0.263	0.003

86	1.292	3.259	0.236	11.893	0.027	0.011
87	0.847	1.841	0.295	7.225	0.121	0.004
88	0.787	1.442	0.472	6.741	0.131	0.000
89	0.727	1.198	0.660	6.434	0.101	0.000
90	0.705	1.156	0.601	5.909	0.143	0.000
91	1.389	3.818	0.290	15.440	-0.229	0.005
92	1.222	2.853	0.283	11.136	0.073	0.005
93	0.907	1.845	0.312	7.299	0.183	0.003
94	0.785	1.450	0.547	7.316	0.057	0.000
95	0.718	1.227	0.730	7.025	0.023	0.000
96	1.234	3.149	0.286	12.563	-0.113	0.005
97	1.134	2.629	0.263	9.976	0.093	0.007
98	0.844	1.702	0.307	6.658	0.194	0.004
99	0.778	1.470	0.544	7.438	0.041	0.000
100	1.266	3.177	0.279	12.536	-0.060	0.006
101	1.098	2.638	0.286	10.382	0.018	0.005
102	0.838	1.726	0.362	7.410	0.071	0.001
103	1.306	3.306	0.324	13.914	-0.150	0.003
104	0.994	2.276	0.346	9.718	-0.028	0.002
105	1.228	3.440	0.360	15.336	-0.381	0.001

3.3.5. Spruce site statistics

Table S5 – Summary of the model statistics (MAE, RMSE, R^2_{adj}, Slope, Intercept and P-value) for each scenario for the spruce dominated sites. Highlighted in red are the two best performing scenarios.

Scenario	MAE	RMSE	R^2_{adj}	Slope	Intercept	P-Value
1	2.675	2.865	0.518	0.577	2.788	0.000
2	2.617	3.080	0.273	0.472	2.556	0.006
3	2.841	3.735	0.028	0.238	2.852	0.216
4	2.752	3.784	-0.004	0.175	2.822	0.350
5	2.660	3.799	-0.027	0.116	2.657	0.527
6	2.630	3.808	-0.033	0.096	2.578	0.597
7	2.653	3.861	-0.041	0.064	2.569	0.721
8	2.734	3.925	-0.045	0.039	2.670	0.830
9	2.747	3.964	-0.047	0.026	2.652	0.886
10	2.774	4.000	-0.047	0.026	2.711	0.889
11	2.868	4.085	-0.048	0.003	2.817	0.989
12	2.944	4.184	-0.047	-0.010	2.906	0.960
13	2.992	4.235	-0.047	-0.014	2.969	0.943
14	3.067	4.279	-0.047	-0.020	3.068	0.921
15	2.077	2.834	0.286	0.533	1.765	0.005
16	1.780	2.517	0.303	0.429	1.525	0.004
17	1.794	2.629	0.211	0.298	1.561	0.016
18	1.879	2.915	0.080	0.205	1.583	0.103
19	1.967	3.081	0.016	0.141	1.520	0.257
20	1.959	3.119	-0.001	0.115	1.465	0.336
21	1.965	3.155	-0.016	0.092	1.470	0.425
22	1.967	3.190	-0.023	0.079	1.455	0.481
23	1.996	3.228	-0.029	0.071	1.502	0.541
24	2.015	3.246	-0.028	0.074	1.516	0.534
25	2.081	3.286	-0.036	0.056	1.570	0.632
26	2.058	3.272	-0.033	0.064	1.580	0.587
27	2.088	3.302	-0.035	0.061	1.632	0.617
28	1.745	2.595	0.254	0.401	1.535	0.008
29	1.388	2.267	0.393	0.416	0.942	0.001
30	1.471	2.516	0.284	0.280	0.944	0.005
31	1.604	2.755	0.152	0.192	0.947	0.037
32	1.701	2.942	0.057	0.123	0.958	0.142
33	1.717	2.997	0.037	0.104	0.917	0.189
34	1.743	3.039	0.020	0.089	0.915	0.244

35	1.777	3.099	-0.006	0.069	0.952	0.363
36	1.783	3.099	-0.005	0.071	0.937	0.358
37	1.765	3.091	-0.003	0.071	0.954	0.342
38	1.768	3.091	-0.001	0.073	0.951	0.335
39	1.796	3.092	-0.004	0.075	0.995	0.348
40	1.336	2.311	0.370	0.368	0.982	0.001
41	1.341	2.437	0.348	0.325	0.653	0.002
42	1.377	2.532	0.420	0.252	0.562	0.000
43	1.527	2.826	0.244	0.151	0.609	0.010
44	1.574	2.942	0.153	0.112	0.637	0.037
45	1.586	3.020	0.094	0.091	0.627	0.084
46	1.597	3.059	0.072	0.080	0.619	0.115
47	1.618	3.084	0.060	0.073	0.613	0.137
48	1.629	3.116	0.033	0.062	0.637	0.201
49	1.637	3.127	0.029	0.060	0.622	0.211
50	1.638	3.094	0.060	0.074	0.606	0.136
51	1.296	2.492	0.314	0.308	0.651	0.003
52	1.263	2.595	0.352	0.250	0.470	0.002
53	1.405	2.739	0.387	0.183	0.445	0.001
54	1.492	2.923	0.286	0.121	0.481	0.005
55	1.519	3.039	0.225	0.091	0.451	0.013
56	1.534	3.096	0.162	0.078	0.442	0.033
57	1.567	3.138	0.123	0.065	0.448	0.056
58	1.575	3.163	0.095	0.059	0.443	0.083
59	1.561	3.139	0.118	0.067	0.452	0.060
60	1.581	3.155	0.111	0.062	0.457	0.067
61	1.235	2.656	0.333	0.233	0.437	0.002
62	1.373	2.857	0.218	0.170	0.405	0.014
63	1.429	2.935	0.231	0.127	0.429	0.012
64	1.476	3.034	0.300	0.095	0.397	0.004
65	1.518	3.103	0.243	0.079	0.375	0.010
66	1.523	3.161	0.233	0.068	0.354	0.011
67	1.519	3.142	0.275	0.075	0.334	0.006
68	1.529	3.178	0.211	0.065	0.340	0.016
69	1.541	3.213	0.207	0.057	0.328	0.017
70	1.392	2.868	0.234	0.168	0.380	0.011
71	1.450	3.015	0.111	0.120	0.430	0.066
72	1.405	3.068	0.106	0.095	0.397	0.071
73	1.441	3.104	0.207	0.081	0.356	0.017
74	1.485	3.109	0.331	0.088	0.287	0.002

75	1.497	3.166	0.377	0.077	0.260	0.001
76	1.529	3.220	0.300	0.062	0.268	0.004
77	1.531	3.219	0.309	0.065	0.249	0.003
78	1.464	3.031	0.092	0.115	0.447	0.086
79	1.481	3.105	0.054	0.096	0.413	0.149
80	1.422	3.093	0.067	0.094	0.394	0.123
81	1.422	3.091	0.194	0.097	0.289	0.020
82	1.465	3.124	0.301	0.087	0.264	0.004
83	1.508	3.193	0.361	0.071	0.246	0.001
84	1.539	3.229	0.327	0.063	0.234	0.003
85	1.464	3.129	0.039	0.084	0.430	0.183
86	1.500	3.162	0.017	0.084	0.429	0.255
87	1.439	3.105	0.066	0.103	0.357	0.125
88	1.441	3.119	0.152	0.088	0.303	0.037
89	1.488	3.162	0.282	0.079	0.247	0.005
90	1.523	3.217	0.337	0.067	0.226	0.002
91	1.506	3.157	0.020	0.086	0.427	0.241
92	1.483	3.141	0.035	0.092	0.394	0.196
93	1.449	3.106	0.070	0.102	0.352	0.118
94	1.429	3.121	0.148	0.090	0.289	0.040
95	1.500	3.186	0.246	0.074	0.240	0.009
96	1.471	3.126	0.040	0.095	0.392	0.182
97	1.480	3.109	0.044	0.102	0.390	0.170
98	1.426	3.102	0.085	0.101	0.326	0.096
99	1.454	3.164	0.112	0.078	0.286	0.065
100	1.480	3.128	0.043	0.100	0.381	0.173
101	1.470	3.127	0.055	0.094	0.363	0.146
102	1.439	3.156	0.055	0.086	0.327	0.145
103	1.458	3.123	0.061	0.094	0.358	0.134
104	1.450	3.156	0.044	0.086	0.347	0.170
105	1.471	3.168	0.036	0.079	0.362	0.191

3.3.6. Scenario-specific model performance for the spruce sites with no bark beetle submodel (ForClim v4.1)

Table S6 – – Summary of model statistics (MAE, RMSE, R^2_{adj}, Slope, Intercept and P-value) for each scenario for the spruce-dominated sites. In this case, the bark beetle routine was switched off. Highlighted in red are the two best soil moisture scenarios selected as best ones in the bark beetle simulations.

Scenario	MAE	RMSE	R^2_{adj}	Slope	Intercept	P-Value
1	1.472	2.423	0.321	0.345	0.816	0.003
2	1.691	2.814	0.093	0.142	1.133	0.085
3	2.075	3.125	-0.010	0.101	1.752	0.384
4	2.173	3.300	-0.028	0.084	1.819	0.530
5	2.190	3.429	-0.043	0.042	1.767	0.751
6	2.216	3.523	-0.048	0.000	1.745	0.998
7	2.241	3.553	-0.047	0.011	1.797	0.938
8	2.311	3.650	-0.047	-0.014	1.862	0.920
9	2.339	3.664	-0.046	-0.025	1.866	0.860
10	2.325	3.662	-0.046	-0.022	1.906	0.874
11	2.363	3.700	-0.046	-0.026	1.942	0.859
12	2.389	3.715	-0.047	-0.017	2.019	0.912
13	2.456	3.813	-0.044	-0.041	2.064	0.788
14	2.486	3.868	-0.043	-0.050	2.110	0.752
15	1.728	3.261	-0.015	0.109	0.955	0.422
16	1.692	2.831	0.090	0.161	1.047	0.089
17	1.626	2.836	0.104	0.168	0.970	0.073
18	1.754	2.986	0.031	0.115	1.039	0.207
19	1.785	3.117	-0.016	0.065	1.004	0.424
20	1.816	3.184	-0.035	0.039	1.025	0.621
21	1.823	3.222	-0.039	0.032	1.005	0.685
22	1.836	3.247	-0.043	0.024	1.000	0.756
23	1.854	3.234	-0.042	0.027	1.034	0.736
24	1.907	3.320	-0.047	0.007	1.093	0.930
25	1.912	3.322	-0.047	0.006	1.082	0.948
26	1.946	3.344	-0.048	-0.002	1.145	0.984
27	1.937	3.345	-0.048	-0.002	1.161	0.981
28	1.820	3.189	-0.008	0.125	1.220	0.374
29	1.511	2.700	0.255	0.214	0.580	0.008
30	1.506	2.794	0.229	0.174	0.585	0.012
31	1.553	2.957	0.123	0.120	0.610	0.056
32	1.589	3.089	0.047	0.075	0.609	0.164
33	1.627	3.188	-0.004	0.047	0.617	0.350
34	1.604	3.176	0.012	0.053	0.575	0.273

35	1.649	3.224	-0.023	0.035	0.626	0.483
36	1.623	3.208	-0.013	0.040	0.609	0.407
37	1.657	3.258	-0.039	0.020	0.654	0.674
38	1.664	3.248	-0.030	0.031	0.642	0.554
39	1.682	3.263	-0.038	0.022	0.680	0.671
40	1.495	2.648	0.275	0.232	0.576	0.006
41	1.420	2.712	0.325	0.213	0.393	0.003
42	1.447	2.863	0.306	0.154	0.415	0.004
43	1.491	3.033	0.206	0.101	0.423	0.017
44	1.545	3.157	0.095	0.065	0.424	0.083
45	1.555	3.200	0.065	0.053	0.424	0.127
46	1.541	3.234	0.053	0.046	0.396	0.149
47	1.541	3.224	0.056	0.045	0.411	0.143
48	1.548	3.222	0.038	0.040	0.428	0.187
49	1.543	3.231	0.032	0.038	0.421	0.203
50	1.570	3.267	-0.001	0.030	0.435	0.333
51	1.400	2.712	0.296	0.217	0.377	0.004
52	1.381	2.851	0.178	0.179	0.409	0.026
53	1.391	2.947	0.235	0.127	0.374	0.011
54	1.480	3.119	0.188	0.077	0.365	0.022
55	1.532	3.191	0.137	0.061	0.346	0.046
56	1.557	3.271	0.077	0.041	0.324	0.107
57	1.543	3.262	0.112	0.046	0.310	0.066
58	1.562	3.298	0.100	0.038	0.290	0.077
59	1.566	3.301	0.088	0.037	0.307	0.092
60	1.579	3.320	0.073	0.033	0.291	0.113
61	1.365	2.888	0.204	0.172	0.334	0.018
62	1.444	3.016	0.096	0.127	0.401	0.082
63	1.422	3.115	0.067	0.085	0.390	0.124
64	1.502	3.192	0.108	0.060	0.329	0.069
65	1.539	3.265	0.093	0.046	0.278	0.086
66	1.549	3.291	0.133	0.042	0.261	0.049
67	1.576	3.305	0.208	0.043	0.228	0.017
68	1.577	3.340	0.136	0.032	0.237	0.047
69	1.586	3.327	0.175	0.039	0.223	0.027
70	1.443	3.018	0.099	0.125	0.399	0.078
71	1.492	3.182	0.009	0.072	0.425	0.284
72	1.443	3.191	0.025	0.073	0.343	0.226
73	1.497	3.236	0.053	0.053	0.302	0.150
74	1.537	3.289	0.122	0.045	0.237	0.057

75	1.566	3.313	0.204	0.044	0.197	0.018
76	1.596	3.333	0.277	0.042	0.171	0.006
77	1.595	3.344	0.276	0.038	0.187	0.006
78	1.519	3.208	-0.001	0.067	0.426	0.334
79	1.510	3.212	0.007	0.072	0.370	0.293
80	1.467	3.215	0.009	0.069	0.344	0.285
81	1.482	3.245	0.054	0.058	0.256	0.147
82	1.544	3.297	0.149	0.048	0.198	0.039
83	1.591	3.338	0.212	0.044	0.167	0.016
84	1.601	3.344	0.274	0.041	0.166	0.006
85	1.501	3.216	0.003	0.068	0.376	0.315
86	1.540	3.264	-0.015	0.057	0.388	0.419
87	1.496	3.235	0.006	0.071	0.317	0.297
88	1.504	3.272	0.055	0.053	0.230	0.146
89	1.556	3.305	0.151	0.050	0.183	0.038
90	1.597	3.350	0.204	0.039	0.163	0.017
91	1.531	3.262	-0.015	0.056	0.387	0.419
92	1.535	3.267	-0.014	0.060	0.374	0.414
93	1.497	3.266	-0.005	0.061	0.317	0.354
94	1.522	3.301	0.030	0.046	0.232	0.209
95	1.574	3.336	0.123	0.040	0.183	0.056
96	1.540	3.263	-0.012	0.062	0.368	0.397
97	1.534	3.230	-0.004	0.072	0.372	0.353
98	1.464	3.270	0.003	0.060	0.277	0.314
99	1.537	3.318	0.018	0.043	0.219	0.249
100	1.532	3.228	0.005	0.075	0.347	0.305
101	1.480	3.240	0.009	0.068	0.300	0.284
102	1.483	3.301	-0.003	0.056	0.257	0.342
103	1.485	3.262	0.005	0.062	0.295	0.303
104	1.474	3.258	0.008	0.068	0.272	0.292
105	1.496	3.266	0.003	0.062	0.295	0.315

185

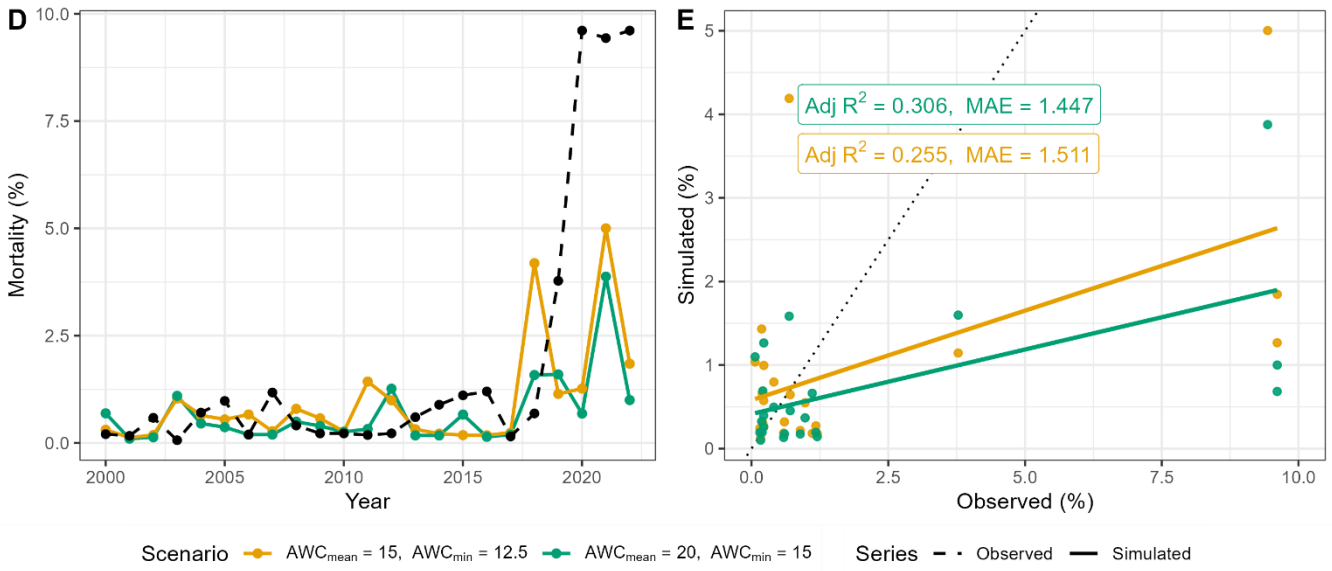

Figure S19 – Simulated and observed mortality rate over time averaged across spruce sites and grouped by soil scenario in the absence of the bark beetle model (ForClim v4.1). Only the two best-performing scenarios are shown.

3.3.7. Sensitivity analysis of kDrSc and P_{bark} parameters

Table S7 - Sensitivity of MAE to PIC parameters. Central-difference slopes of MAE per 1% parameter change for the drought-inciting scaling factor (kDrSc) and baseline outbreak probability (P_{bark}) in scenarios 29 and 42. Slopes are averaged over the ±10% and ±20% perturbation pairs; 95% bootstrap confidence intervals are from resampling years. Negative slopes indicate that increasing the parameter reduces MAE (improved fit). Larger |slope| denotes greater sensitivity.

Scenario	Factor	Direction	Slope (ΔMAE per 1%)	95% CI	Slope
29	kDrSc	↓ MAE (better)	-0.004421	(-0.034152, 0.027718)	0.004421
29	P_{bark}	↑ MAE (worse)	0.000431	(-0.032952, 0.031187)	0.000431
42	kDrSc	↓ MAE (better)	-0.000769	(-0.037759, 0.033127)	0.000769
42	P_{bark}	↑ MAE (worse)	0.000005	(-0.035107, 0.035660)	0.000005

S4 | ForClim 4.1: Predisposing and Inciting factor scheme

4.1. | Overview

ForClim is a forest gap model (Botkin et al., 1972) originally designed to capture the long-term (i.e., decades to centuries) growth, mortality and regeneration of trees in temperate forests of central Europe and account for climate change effects on forest dynamics (Bugmann, 1994, 1996). In gap models, forest dynamics are simulated on small areas ('patches'), usually with a size of 400-1000 m^2, each representing one out of many stochastic realizations that are spatially independent of each other. The soil moisture balance is calculated using a monolayer "bucket" model that stores all incident water until its capacity ("bucket size", kBS) is reached, which corresponds to AWC. The bucket model has a fixed field capacity, beyond which soil moisture cannot increase. This simplification facilitates computations but limits the representation of hydrological processes such as percolation and soil moisture variability above field capacity. For details, cf. Bugmann and Cramer (1998); Bugmann and Solomon (2000).

This bucket model is directly linked to plant dynamics, with tree growth being determined as a species-specific potential (i.e., under optimum conditions) that is reduced via a growth-reduction factor (*GRF,* cf. *Eq. S3*) accounting for light availability (*ALGF*), crown condition (*CLGF*), temperature (*DDGF*) , nitrogen (*SNGF*) and soil moisture (*SMGF*; for details cf. Bugmann & Solomon, 2000;Huber et al., 2020):

$$GRF = \sqrt{CLGF \cdot SNGF \cdot ALGF \cdot SMGF \cdot DDGF} \qquad \textbf{Eq. S3}$$

SMGF depends on the annual drought index (*gDr*) and a species-specific drought tolerance parameter (*kDrTol*). *gDr* is computed at a monthly time step for deciduous species considering the length of the growing season in temperate regions (i.e., April – October), and across the year for evergreen species, provided temperatures are high enough (cf. Bugmann and Cramer, 1998). In this version of ForClim (v4.0.1; Huber et al., 2020), tree mortality from stress is assumed to occur when diameter growth falls below a specific stem diameter increment or a fraction of the maximum increment for several years (Solomon and Shugart, 1989). Thus, *predisposing* stress is assumed to increase the mortality rate, but there is no consideration of *inciting* stress (cf. the PIC scheme).

4.2. | Integrating predisposing and inciting stress factors

To enhance the response of tree growth to environmental extremes (temperature and soil moisture dynamics), we modified the original growth reduction formulation (Huber et al. 2020) by applying Liebig's "law of the minimum" for the temperature (*DDGF*) and soil moisture (*SMGF*) growth factors (Eq. S4; cf. Liebig et al., 1842), rather than multiplying them:

$$GRF = \sqrt{CLGF \cdot SNGF \cdot ALGF} \cdot \min(SMGF, DDGF) \quad \textbf{Eq. S4}$$

The underlying rationale is that in temperate and boreal regions, conditions are typically either dry *or* cold, but not dry *and* cold (cf. Bugmann, 1996). To preserve the species-specific response to environmental stress although the level of GRF is changing due to the use of *Eq.S4* instead of *Eq. S3*, we had to re-estimate a temperature-related species-specific parameter, and we also modified the dynamic formulation of site index, which reflects the response of maximum tree height to temperature and drought and their changes over time. All past formulations of *GRF* together with a sensitivity analysis.

To disentangle predisposing and inciting factors leading to drought-related mortality, we identified short-term (within a year) and long-term (multi-year) stressors linked to drought duration and intensity as well as carbon starvation, as explained below.

First, we accounted for the effect of long-lasting droughts by *a predisposing factor* using a drought memory term (*DrM*; Wang et al., 2012, *Eq. S5*):

$$DrM = \begin{cases} DrM + 1, & gDr > kDrTh \cdot kDrTol_s \\ 0, & else \end{cases} \quad \textbf{Eq. S5}$$

This formulation counts all contiguous years in which drought intensity, represented by the ForClim drought index (*gDr*), exceeds a fraction (*kDrTh*) of the species-specific drought tolerance ($kDrTol_s$). In this manner, we account for the species-specific resistance to multi-annual drought occurrence. To be consistent, we also modified the "slow growth" factor SGr to better mimic the impact of carbon reserves on mortality risk.

Second, to deal with inciting factors we defined drought duration within any given year (*gDrD*, *Eq. S6*) as the ratio of the number of dry months relative to the total number of months *m* of the growing period (for deciduous species, m_{gp}; annual for evergreen species, m_{an}). The algorithm selects those months in which the average temperature (T_m) is above a threshold *kJ* (5.5 °C) while water supply (i.e., transpiration, gE_m, cm) relative to water demand from the soil (*gDm*, cm) is below a threshold *kEg*; i.e., $gE_m/gD_m < kEg$; and $SM_s < kBS$; note that the full documentation of all soil moisture variables can be found in Marano et al. 2025). The term $\mathbb{1}$ in *Eq. S6* represents an indicator function that equals 1 if the condition is yes for a given month, and 0 otherwise.

$$gDrD_{gp} = \frac{1}{m_{gp}} \sum_{m=4}^{10} \mathbb{1}(T_m \geq \text{kJ}) \cdot \mathbb{1}(SM_m < kBS) \cdot \mathbb{1}\left(\frac{gE_m}{gD_m} < \text{kEg}\right)$$

Eq. S6

$$gDrD_{an} = \frac{1}{m_{an}} \sum_{m=1}^{12} \mathbb{1}(T_m \geq \text{kJ}) \cdot \mathbb{1}(SM_m < kBS) \cdot \mathbb{1}\left(\frac{gE_m}{gD_m} < \text{kEg}\right)$$

Third, under conditions of low demand (i.e., in spring and fall) the index of *Eq. S6* would not record any drought, although soil moisture (SM_m) may be limiting e.g. for bud break. Thus, we defined two variables to capture limiting soil moisture levels in spring and fall along with a threshold (parameter *kDu*) for the duration of the drought to define an *inciting* factor for drought stress (*IncFDr; Eq. S7*).

$$IncFDr = \begin{cases} 1, & (SM_{spring} < kREW_{spring} \cdot kBS) \wedge (SM_{fall} < kREW_{fall} \cdot kBS) \wedge gDrD > kDu \\ 0, & else \end{cases}$$

Eq. S7

This formulation for the water deficit in spring and fall is based on the concept of 'relative extractable water' (REW; Breda et al., 1980; Granier et al., 1999). Specifically, the spring component of *IncFDr* reflects the need of trees to mobilize water for bud break and cell division and elongation, while the fall component reflects the need of accumulating carbon reserves for the subsequent year (cf. REW). The threshold *kDu* was set to 0.28, corresponding to two months out of a seven-month growing period (2/7 ≈ 0.28) for broadleaves, and three to four months out of the whole year (3.5/12 ≈ 0.29) for evergreen species, provided that winters are warm enough (cf. Hidy et al., 2012, 2021; Merganičová et al., 2024). The seasonal soil moisture levels (SM_{fall}, SM_{spring}) are calculated for the fall (September to November) and spring (March to May) periods for both evergreen and deciduous species.

Lastly, the overall stress-induced mortality probability (*gPStr*), including carbon memory and integrating predisposing as well as inciting factors, is formulated as follows:

$$gPStr = \begin{cases} kStressP, & SGr > kSGrT \vee (DrM > kSGrT \wedge IncFDr = 1) \\ 0, & else \end{cases}$$

Eq. S8

where $kStressP$ is the stress-induced enhanced mortality probability, SGr is the counter for slow-growth years, and $kSGrT$ indicates the number of stress years that are tolerated until mortality probability may rise, provided that there is an inciting factor (Peltier et al., 2023). The first term of *Eq. S8* (*SGr* condition) captures the probability that a tree may die due to slow growth induced by whatever cause (e.g., insufficient light), whereas the second term (*DrM* and *IncFDr* conditions)

reflects that a string of dry years (predisposing factors) can enhance mortality under a particularly prolonged summer drought when coupled to early- and/or late-season soil moisture depletion (inciting factor).

The ensemble of these features gives rise to ForClim v4.1. Since contributing factors (sensu Manion, 1981) such as insect damage are currently not included, we refer to the concept underlying ForClim v4.1 as the "PI framework", rather than PIC.

All species- and process-specific parameters used in the new drought mortality formulation were set based on literature values, ecological reasoning, or consistently with values used in previous ForClim versions. Importantly, no parameters were calibrated against the empirical data. This ensures that the simulation outcomes reflect the structural behavior of the new formulation rather than fitting to observations. Further material can be found in the manuscript Marano et al. 2025 currently under revision at *Ecosphere*.

References

Anselin, L.: Local Indicators of Spatial Association—LISA, Geographical Analysis, 27, 93–115, https://doi.org/10.1111/j.1538-4632.1995.tb00338.x, 1995.

Botkin, D. B., Janak, J. F., and Wallis, J. R.: Some Ecological Consequences of a Computer Model of Forest Growth, The Journal of Ecology, 60, 849–849, https://doi.org/10.2307/2258570, 1972.

Breda, N., Huc, R., Granier, A., and Dreyer, E.: Temperate forest trees and stands under severe drought: a review of ecophysiological responses, adaptation processes and long-term consequences Nathalie, 28, 389–390, https://doi.org/10.1016/s0034-5288(18)32731-0, 1980.

Bugmann, H.: On the Ecology of Mountainous Forests in a Changing Climate: A Simulation Study, Dissertation, ETH Zurich, 252 pp., 1994.

Bugmann, H. and Cramer, W.: Improving the behaviour of forest gap models along drought gradients, Forest Ecology and Management, 103, 247–263, https://doi.org/10.1016/S0378-1127(97)00217-X, 1998.

Bugmann, H. K. M.: A Simplified Forest Model to Study Species Composition Along Climate Gradients, Ecology, 77, 2055–2074, https://doi.org/10.2307/2265700, 1996.

Bugmann, H. K. M. and Solomon, A. M.: Explaining forest composition and biomass across multiple biogeographical regions, Ecological Applications, 10, 95–114, https://doi.org/10.1890/1051-0761(2000)010[0095:EFCABA]2.0.CO;2, 2000.

Granier, A., Bréda, N., Biron, P., and Villette, S.: A lumped water balance model to evaluate duration and intensity of drought constraints in forest stands, Ecological Modelling, 116, 269–283, https://doi.org/10.1016/S0304-3800(98)00205-1, 1999.

Hidy, D., Barcza, Z., Haszpra, L., Churkina, G., Pintér, K., and Nagy, Z.: Development of the Biome-BGC model for simulation of managed herbaceous ecosystems, Ecological Modelling, 226, 99–119, https://doi.org/10.1016/j.ecolmodel.2011.11.008, 2012.

Hidy, D., Barcza, Z., Hollós, R., Thornton, P. E., Running, S. W., and Fodor, N.: User's Guide for Biome-BGCMuSo 6.1, 2021.

Huber, N., Bugmann, H., and Lafond, V.: Capturing ecological processes in dynamic forest models: why there is no silver bullet to cope with complexity, Ecosphere, 11, https://doi.org/10.1002/ecs2.3109, 2020.

Liebig, J., Playfair, L. P., and Webster, J. W.: Chemistry in its application to agriculture and physiology, J. Owen, Cambridge, https://doi.org/10.5962/bhl.title.30425, 1842.

Manion, P. D.: Tree disease concepts, Prentice-Hall, Inc., 1981.

Marano, G., Hiltner, U., Meusburger, K., Hands, T., and Bugmann, H.: Predicting drought-induced tree mortality in Swiss beech forests hinges upon predisposing and inciting factors, bioRxiv [preprint], https://doi.org/10.64898/2025.12.15.694299, 2025.

Merganičová, K., Merganič, J., Dobor, L., Hollós, R., Barcza, Z., Hidy, D., Sitková, Z., Pavlenda, P., Marjanovic, H., Kurjak, D., Bošel'a, M., Bitunjac, D., Ostrogović Sever, M. Z., Novák, J., Fleischer, P., and Hlásny, T.: The biogeochemical model Biome-BGCMuSo v6.2 provides plausible and accurate simulations of the carbon cycle in central European beech forests, Geosci. Model Dev., 17, 7317–7346, https://doi.org/10.5194/gmd-17-7317-2024, 2024.

Moran, P. A. P.: Notes on continuous stochastic phenomena, Biometrika, Volume 37, 17–23, https://doi.org/10.1093/biomet/37.1-2.17, 1950.

Peltier, D. M. P., Carbone, M. S., McIntire, C. D., Robertson, N., Thompson, R. A., Malone, S., LeMoine, J., Richardson, A. D., McDowell, N. G., Adams, H. D., Pockman, W. T., and Trowbridge, A. M.: Carbon starvation following a decade of experimental drought consumes old reserves in Pinus edulis, New Phytologist, https://doi.org/10.1111/nph.19119, 2023.

Solomon, A. M. and Shugart, H. H.: Vegetation dynamics and Global change, https://doi.org/10.1017/CBO9781107415324.004, 1989.

Wang, W., Peng, C., Kneeshaw, D. D., Larocque, G. R., and Luo, Z.: Drought-induced tree mortality: Ecological consequences, causes, and modeling, Environmental Reviews, 20, 109–121, https://doi.org/10.1139/a2012-004, 2012.